

# Numerical Simulation of Nonlinear Waves about a Submerged Hydrofoil

Kuk-Jin Kang

Korea Research Institute of Ships and Ocean Engineering

## Introduction

The wave generation due to the presence of a body moving at steady forward speed beneath a free surface has been the subject of extensive research work in marine hydrodynamics. Duncan(1983) obtained experimental results for the breaking and non-breaking wave resistance of a two-dimensional hydrofoil. Thereafter many researchers have tried to simulate the steady and breaking waves at similar conditions, and some of the results are summarized briefly here. Coleman(1986) tried to simulate the breaking process for the foil using finite-difference method by the application of an artificial pressure distribution on the free surface and a Kutta condition at the trailing edge, and showed rather phase-shifted and over-predicted wave profiles. Tzabiras(1991) calculated the wave pattern for the foil using an NS solver with a  $k-\epsilon$  turbulence model, and showed rather under-predicted results and much different wave patterns for the two kinds of grid system. Liu(1991) also calculated the same case using an NS solver with a zero-equation turbulence model, but did not show good agreement with experiments. Hino(1993) introduced the finite-volume method with an unstructured grid for free surface flow simulations. The method was based on the Euler equations and showed good results. However, he failed to simulate the breaking wave. The objective of the present work is to develop an accurate finite-volume method based on the Euler equations and to apply the scheme to the free surface problem around a submerged hydrofoil, and further to try to simulate the process of breaking wave numerically.

## Numerical Procedures

The governing equations are the two-dimensional incompressible continuity equation and the Euler equations, expressed in the free surface fitted curvilinear coordinate system  $(\xi_i, \tau)$ ,  $t = \tau$  as follows:

$$\frac{1}{J} \frac{\partial}{\partial \xi^i} (A_k^i u_k) = 0$$
$$\frac{\partial u_i}{\partial \tau} + \frac{1}{J} \frac{\partial}{\partial \xi^j} \left\{ u_i \frac{\partial \xi_i}{\partial t} + A_k^j (u_i u_k + \phi \delta_{ik}) \right\} = 0$$

where,  $A_k^j$  : surface area of cell,  $\phi = \psi + \frac{y}{Fn^2}$ ,  $Fn = \frac{U}{\sqrt{gL}}$

The finite-volume formulation is adapted to discretize the fluid domain and a staggered grid is used to define the velocity and pressure. Time marching procedure is used to solve the unsteady problem, where the convection terms are approximated by a 3rd-order upwind scheme and a 2nd-order central differencing scheme is used for the other spatial derivatives. Pressure and velocity fields are calculated by the simultaneous iteration method. A H-H type grid system is adapted for the submerged hydrofoil and generated by Steger's method(1979). Grids move vertically in an Eulerian manner.

## Numerical Treatment of Boundary Conditions

### Body boundary condition

The Euler solver requires the free-slip condition on the body boundary. That is, the normal velocity component ( $V_1$ ) should be zero and the tangential velocity component ( $U_1$ ) is set to equal to the most adjacent one ( $U_2$ ) on the body. From these relations, velocity components ( $u_1, v_1$ ) on the body are calculated.

### Free surface condition

$$\text{Dynamic condition : } \phi = p_o + \frac{h}{Fn^2} \quad \text{on } y = h$$

$$\text{Kinematic condition : } \frac{\partial h}{\partial t} + u \frac{\partial h}{\partial \xi} \frac{\partial \xi}{\partial x} - v = 0.$$

The free surface shape is updated in a time-marching manner. A 3rd-order upwind scheme is used for  $h_\xi$  and a 2nd-order central differencing scheme is used for the  $\xi_x$ . The velocity on the free surface is extrapolated from inside in such way that the velocity gradient in the normal direction is zero.

### Far field conditions

$$\text{At the inflow : } u = 1, \quad v = 0, \quad \phi = 0, \quad h = 0$$

$$\text{At the bottom : } u = 1, \quad v = 0, \quad \phi = 0$$

At the outflow, a zero-extrapolation method is used for the velocity and pressure. The artificial wave damping method proposed by Hino(1993) is used to prevent the reflection of waves to the solution domain.

## Computational Results

The numerical procedure was applied to free surface flow simulations around a submerged NACA0012 hydrofoil section at  $5^\circ$  incidence angle, which was tested experimentally in detail by Duncan(1983). For the computations, the mid-chord of the foil is placed at 0.862 chord lengths above the bottom boundary which is a geometrically similar arrangement to the experiments. Parameters are non-dimensionalized by the chord length  $L$  and the leading edge is located at  $x = -0.25$ . Computational conditions which correspond to the experiments are summarized in the table below.

Fn	Submerged Depth (d/L)			x-domain of Computation
	Breaking Region	Transition Region	Non-breaking Reg.	
0.425	0.754		0.84	$-7 \leq x \leq 6.25$
0.567	0.911	0.951	1.034	$-7 \leq x \leq 6.25$
0.709	0.951		1.034	$-7 \leq x \leq 10.0$

In Fig. 1 the computed wave height is compared with the experimental data by Duncan and shows good agreement at  $Fn=0.567$ ,  $d/L=0.951$  and  $1.034$ . In Fig. 2 the process of wave-breaking is shown at  $Fn=0.425$  and  $d/L=0.754$ . According to the results, after the wavetrain has been fully developed, wave-breaking starts from the second wave crest and propagates to the first wave and finally the first wave is overturned. In Fig. 3 the process of wave-breaking is shown at  $Fn=0.567$  and  $d/L=0.911$ . The features of the wave-breaking is quite different from those above. The first wave is growing up rapidly and overturned. In Fig. 4 the process of wave-breaking is shown at  $Fn=0.7087$  and  $d/L=0.951$ . The wave-breaking pattern is also quite different from the other cases. After the second wave becomes steep, the wave starts to collapse, but not to propagate to the first wave, and then it restarts to grow up. This phenomenon may represent the transient or sub-breaking wave.

### Concluding Remarks

In the present study, a finite-volume method with a moving grid system was developed. The computed results for a submerged hydrofoil show good agreement with experimental data. Three kinds of wave-breaking processes could be observed in the simulation results. Further extensions of this method are the inclusion of viscous effects, a more efficient numerical scheme and generalization to three dimensions.

### Acknowledgment

This work was done while the author stayed at Chalmers University of Technology (CTH) as a visiting research fellow. He is grateful to the Korea Research Institute of Ships & Ocean Engineering, the Korea Science & Engineering Foundation and the Swedish Institute for the support during his stay at CTH. The author would like to thank Prof. Lars Larsson of CTH for having discussions about the computational results and offering facilities for the calculation.

### References

- Coleman R. M., "Nonlinear Calculation of Breaking and Non-Breaking Waves Behind a Two-Dimensional Hydrofoil", 16th Sym. on Naval Hydro., Berkeley, USA, July 1986.
- Duncan J. H., "The breaking and non-breaking wave resistance of a two-dimensional hydrofoil", J. Fluid Mech. vol. 126, 1983.
- Hino T., "A Finite-Volume Method with Unstructured Grid for Free Surface Flow Simulations", 6th Int. Conf. on Numerical Ship Hydro, Iwoa, USA, Aug. 1993.
- Liu H. and Ikehata M., "Computation of Free Surface Viscous Flow with High Reynolds Number around a Submerged Hydrofoil", 2nd Osaka Int. Colloquium on Viscous Fluid Dynamics in Ship and Ocean Tech., Japan, Sep. 1991.
- Steger J. L. and Sorenson R. L., "Automatic Mesh-Point Clustering Near a Boundary in Grid Generation with Elliptic Partial Differential Equations", JCP, vol. 33, 1979.
- Tzabiras G. and Ventikos Y., "Calculation of the Wave Pattern Generated by a 2D Submerged Hydrofoil : A Navier-Stokes Approach", Math. and Numerical Aspects of Wave Propagation Phenomena, Chapter 40, April 1991.

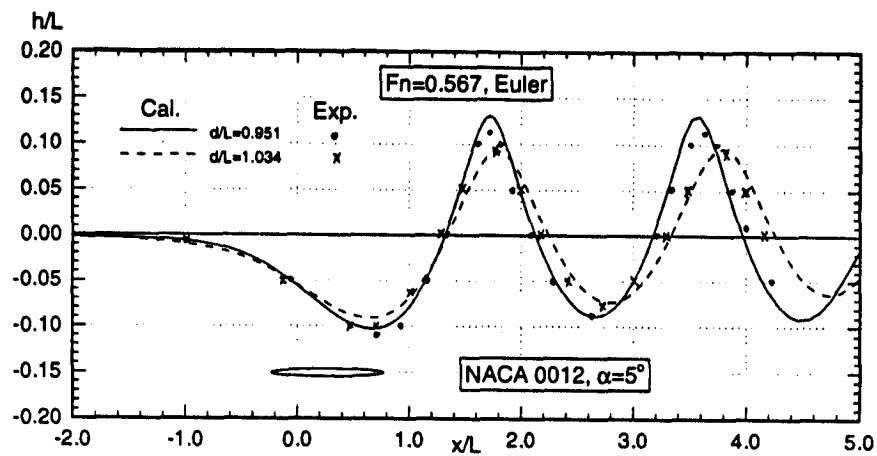


Fig. 1 Comparison of Wave Profiles at  $d/L=0.951, 1.034$

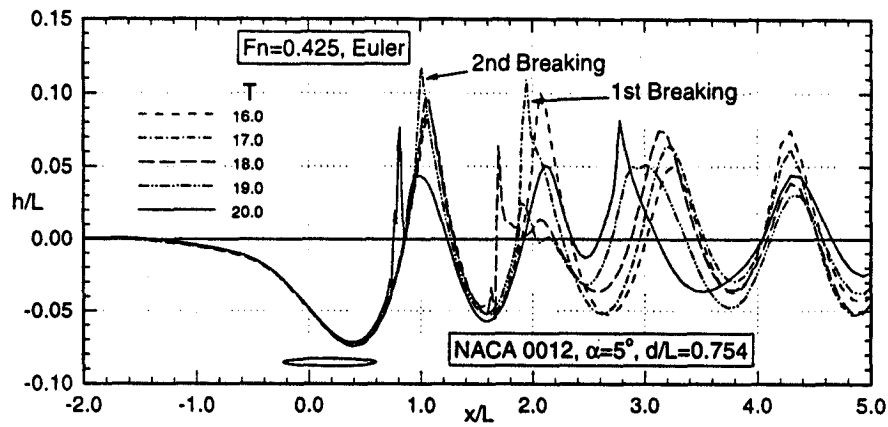


Fig. 2 Computed Wave Profiles ( $Fn=0.425, d/L=0.754$ )

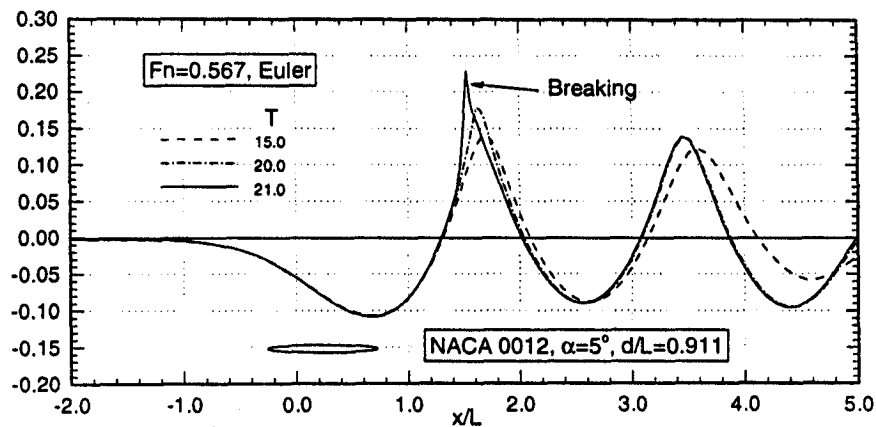


Fig. 3 Computed Wave Profiles ( $Fn=0.567, d/L=0.911$ )

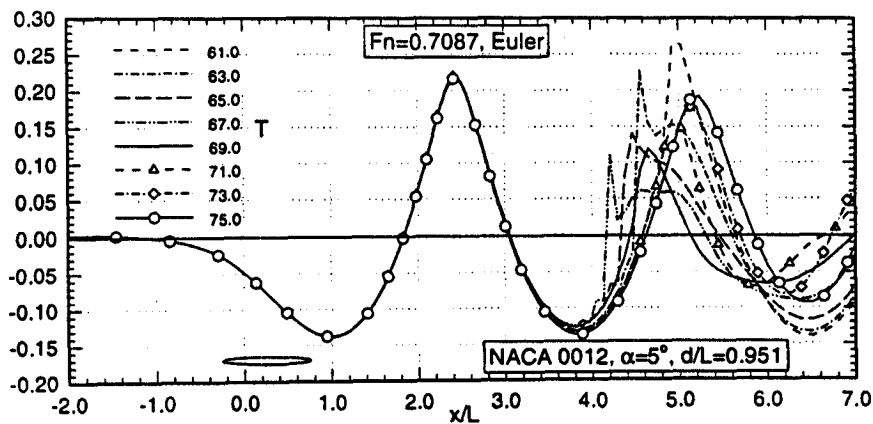


Fig. 4 Computed Wave Profiles ( $Fn=0.7087, d/L=0.951$ )

## DISCUSSION

**Schultz:** I don't understand your dynamic free-surface condition. It seems steady. What is  $p_0$ ? I also fail to understand the  $\partial v / \partial n = 0$  condition on the free surface.

**Kang:**  $p_0$  is set to zero on the free surface. The existence of a boundary layer very near to the free surface is neglected. So, the velocity components can be extrapolated using interior values. In my case, I used the zero-extrapolation method.

**Armenio:** Can your computation continue after breaking wave condition has been reached?

**Kang:** It is impossible to continue the wave calculation after the breaking wave condition. This numerical scheme can solve the single value problem only because grids move vertically in an Eulerian manner. However, it is possible to continue the unsteady wave calculation if the waves are not overturned, as shown in Fig.4.